Journal of Magnetic Resonance 298 (2019) 107–114

Contents lists available at ScienceDirect

Journal of Magnetic Resonance

journal homepage: www.elsevier.com/locate/jmr

Proton detection of carbon-carbon couplings in symmetrical molecules: Analytical explanation, SYMONA pulse sequence

Vratislav Blechta *, Jan Sýkora

Institute of Chemical Process Fundamentals of the CAS, v. v. i., Rozvojova 135, 165 02 Prague 6, Czech Republic

ARTICLE INFO

Article history:
Received 11 July 2018
Revised 26 November 2018
Accepted 3 December 2018
Available online 5 December 2018

Keywords:
NMR
Carbon-carbon coupling
Strong coupling
Equivalent carbons
Proton detection
2QHMBC
SYMONA

ABSTRACT

The approach to the measurement of one-bond indirect spin–spin coupling constants between equivalent nuclei was revisited. The analytical formulas for development of the density matrix of strongly coupled symmetrical HC-C′H′ spin systems were derived and the optimal duration of polarization delay in the original 2QHMBC pulse sequence is discussed. Based on the analytical formulas a new version of a robust indirect detection experiment, called SYMONA (SYmmetrical MOlecules Natural Abundance double-quantum experiment), was proposed for carbon–carbon coupling constants detection in symmetrical molecules. Additionally, application of the SYMONA experiment to more complicated spin systems than isolated HC-C′H′ is discussed.

1. Introduction

Indirect spin-spin coupling constants represent a unique source of information about the electron distribution between involved nuclei. These couplings can be correlated to bond-related structural parameters like bond distance, bond angle, the fraction of σ character in the bond and so on. Generally speaking, couplings reflect the bonding environment [1].

In order to measure the carbon-carbon coupling constants, the INADEQUATE [2] experiment was introduced. This rather insensitive NMR experiment relies on direct observation of the target nucleus. Later, the indirectly detected experiment – ADEQUATE [3] was proposed for measurement of couplings between protonated carbons. The sensitivity of this experiment is several times higher than the sensitivity of the original pulse sequence. However, the coupling between quaternary carbon atoms cannot be detected by this method. A specific experimental challenge is represented by the determination of coupling between nuclei of similar chemical shift or even symmetrically equivalent nuclei. Coupling constants between such atoms are difficult to measure due to the collapse of the NMR signal by a symmetry-equivalent pair into a single line. The asymmetry needed for measurement can be induced e.g. via deuterium labelling or orientation in chiral media [4]. However, there were also several attempts to measure these couplings directly and at natural abundance. There are two available pulse sequences (see the next paragraph) which were primarily designed for coupling determination in dichloroethene possessing the simplest CH-C'H' spin system. Both methods utilize the signal splitting induced by one-bond carbon-proton coupling that can create effective chemical shift differences [5] between equivalent nuclei and thus remove the chemical shift degeneracy at least for part of the experimental coherences.

The older method is the standard 1D INADEQUATE but without decoupling during preparation and acquisition periods [6]. The method was tested on both *cis*- and *trans*-dichloroethene. The acquired spectrum contained information on the carbon-carbon coupling constant. However, for the precise determination of coupling a simulation of spectrum was necessary. The proposed pulse sequence was subsequently used in number of papers discussing e.g. the comparison of the σ bond contribution in *cis*- and *trans*-isomers in symmetrical alkenes [7] or the aromaticity in the series of five-membered heterocycles [8]. The method was also utilized in the study of symmetric disilanes for determination of $^{1}J(^{29}Si^{29}Si)$ [9].

The second method is a modified, indirectly detected 2QHMBC experiment [10] which utilizes the polarization transfer from protons to coherences containing carbon two-spin coherences [11]. The polarization transfer is followed by a carbon double-quantum gradient filter and acquisition period without carbon

* Corresponding author.
E-mail address: blechta@icpf.cas.cz (V. Blechta).

https://doi.org/10.1016/j.jmr.2018.12.002
1090-7807/

decoupling. The method was tested on *trans*-dichloroethene and the paper also proposed an optimal experimental setup. However, the expression for the amplitude of double-quantum carbon coherences in the 2QHMBC experiment is more complicated than originally assumed. The work was extended afterwards for a series of symmetrical strained alkenes [12].

In this paper we focus on more sensitive 2QHMBC experiment. We offer analytical formulas for development of a density matrix of strongly coupled symmetrical HC-C'H' spin systems and discuss the optimal duration of polarization delay in the pulse sequence. Based on the analytical formulas a new version of a robust indirect detection experiment, called SYMONA (SYmmetrical MOlecules Natural Abundance double-quantum experiment), is proposed for carbon-carbon coupling constant detection between equivalent nuclei. Additionally, utilization of the SYMONA experiment with more complicated spin systems is discussed.

The formalism derived here might be helpful also in NMR hyperpolarized substances [13] where extremely long-living singlet states [14] are designed for utilization in experiments *in vivo*. In some cases, the singlet states are generated on symetrical AA′XX′ spin systems, usually HH′13C13C′ [15,16,17] or HH′15N15N′ [18], which are basically identical with HC-C′H′ system discussed within this work.

2. Results and discussion

2.1. 2QHMBC experiment

The 2QHMBC pulse sequence adopted for detection of coupling constants between equivalent nuclei is composed of three parts (Fig. 1). The first part utilizes polarization transfer from protons to coherences containing carbon two-spin coherences ($C_zC'_z$). The second part starts with the first carbon pulse which partially transfers the carbon two-spin coherences to double-quantum ones, namely $\left(C_xC'_x - C_yC'_y\right)\left(H_x + H'_x\right)$ and $\left(C_xC'_x - C_yC'_y\right)2\left(H_yH'_z + H'_yH_z\right)$. The rest of the preparation period is essentially a carbon double-quantum gradient filter closed by a second carbon 90-degree pulse which partially transfers the carbon double-quantum coherences back to zero-quantum ones. The third part is formed by the acquisition without carbon decoupling. In practice, it is convenient to focus only on compounds possessing directly coupled carbons with attached protons that are not coupled to any other proton: the HC-C′H′ system. For correct definition of the Hamiltonian see Supporting Information (Appendices, Appendix A, Eq. (A1)). Possible influence of remote protons will be shortly discussed for experimental examples.

The originally proposed value for polarization delay (*d2*) is equal to $1/(2{}^1J(C,H))$ which is usually used for polarization transfer in weakly coupled spin systems. In fact, this assumption is misleading because the HC-C′H′ symmetric spin system is not a weakly coupled system. The correct expression for the amplitude of double-quantum carbon coherences in the 2QHMBC experiment after the first carbon pulse is given in Eq. (1). The whole derivation can be found in Supplementary material 1 (Appendices, Appendix B).

$$\left(C_xC'_x - C_yC'_y\right)\left(H_x + H'_x\right)\left[\cos\left(\pi({}^1J_{CH} + {}^2J_{CH})t\right) - cos(\lambda^s t)cos\left(\pi({}^1J_{CC} + {}^3J_{HH})t\right) - s2^s sin(\lambda^s t)sin\left(\pi({}^1J_{CC} + {}^3J_{HH})t\right)\right] + \tag{1}$$

$$\left(C_xC'_x - C_yC'_y\right)2\left(H_yH'_z + H'_yH_z\right)\left[cos(\lambda^s t)sin\left(\pi({}^1J_{CC} + {}^3J_{HH})t\right) - s2^s sin(\lambda^s t)cos\left(\pi({}^1J_{CC} + {}^3J_{HH})t\right)\right]$$

$$\lambda^s = \pi\sqrt{\left(({}^1J_{CH} - {}^2J_{CH})^2 + ({}^1J_{CC} + {}^3J_{HH})^2\right)}, s2^s = \pi\frac{|{}^1J_{CC} + {}^3J_{HH}|}{\lambda^s}.$$

In Eq. (1), ${}^1J_{CC}$ and ${}^3J_{HH}$ stand for one-bond carbon-carbon and three-bond proton-proton couplings, respectively. This formula and the following text are valid for any values of coupling constants. Therefore they include *n*-bond distant carbons with ${}^1J_{CC}$, ${}^2J_{CH}$ and ${}^3J_{HH}$ substituted by ${}^nJ_{CC}$, ${}^{n+1}J_{CH}$ and ${}^{n+2}J_{HH}$ in Eq. (1). The originally expected maximum for time $t = 1/2{}^1J(C,H)$, supposes a time dependence equal to $sin(\pi{}^1J_{CH}t)$. Note that the polarization transfer delay *t* corresponds to *d2* delay in the pulse sequence (Fig. 1). Obviously, the real time development given in Eq. (1) is much more complicated than originally assumed, as the term in Eq. (1) depends on frequencies $({}^1J_{CH} + {}^2J_{CH})$, $({}^1J_{CC} + {}^3J_{HH})$ and λ^s. Moreover, there are two different carbon double-quantum coherences: $\left(C_xC'_x - C_yC'_y\right)\left(H_x + H'_x\right)$ and $\left(C_xC'_x - C_yC'_y\right)2\left(H_yH'_z + H'_yH_z\right)$, each with its own buildup of the amplitudes (Fig. 2). The buildup curves were calculated for typical aliphatic (${}^1J(C,C) \sim 40$ *Hz*, ${}^1J(C,H) \sim 140$ *Hz*, ${}^3J(H,H) \sim 8$ *Hz*) and aromatic systems (${}^1J(C,C) \sim 60$ *Hz*, ${}^1J(C,H) \sim 160$ *Hz*, ${}^3J(H,H) \sim 8$ *Hz*).

Obviously, the double-quantum carbon coherences provided maxima at positions very different from the original assumption. The 2QHMBC signal maximum for $\left(C_xC'_x - C_yC'_y\right)\left(H_x + H'_x\right)$ coherence can be estimated from the approximate formula

$$\left(1 - \cos\left(\pi({}^1J_{CC} + {}^3J_{HH})t\right)\right)\cos\left(\pi{}^1J_{CH}t\right), \tag{1a}$$

If it is supposed that $\lambda^s \cong {}^1J_{CH}$ and ${}^2J_{CH} \cong 0$ at least for short *t* delay. Value of $s2^s$ is typically less than 0.4 and the product $s2^s sin(\lambda^s t)sin\left(\pi({}^1J_{CC} + {}^3J_{HH})t\right)$ is close to zero since condition $sin(\lambda^s t) \cong sin\left(\pi({}^1J_{CC} + {}^3J_{HH})t\right) \cong 0$ is satisfied when a maximum amplitude of $\left(C_xC'_x - C_yC'_y\right)\left(H_x + H'_x\right)$ coherence is approached. The maximum achievable amplitude for this coherence is 2 if a suitable combination of coupling constants occurs. The maximum achievable amplitude for $\left(C_xC'_x - C_yC'_y\right)2\left(H_yH'_z + H'_yH_z\right)$ appears to be only 1. Therefore, the experimental setup should follow the buildup of $\left(C_xC'_x - C_yC'_y\right)\left(H_x + H'_x\right)$ coherence primarily.

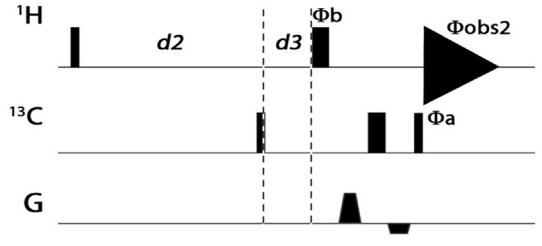

Fig. 1. 2QHMBC pulse sequences for proton detection of carbon-carbon couplings in symmetric molecules [10]. For phases Φobs2, Φb and d2, d3 delays see Berger's paper [10]. Gradient amplitudes are in ratio 3.02:−1.

2.2. SYMONA experiment

Here, we propose a different pulse sequence, which is shown in its simplified version in Fig. 3a. The preparation period consists of $(t/2 - R_H - t/2)$ polarization transfer segment of the total length $1/(J_{CC} + J_{HH})$ for creation of two-spin carbon coherence where R_H is the proton inversion pulse. The main task of the proton R_H pulse is to refocus heteronuclear couplings. R_H can in principle be substituted by the carbon inversion pulse at the cost of losing proton chemical shift refocusing.

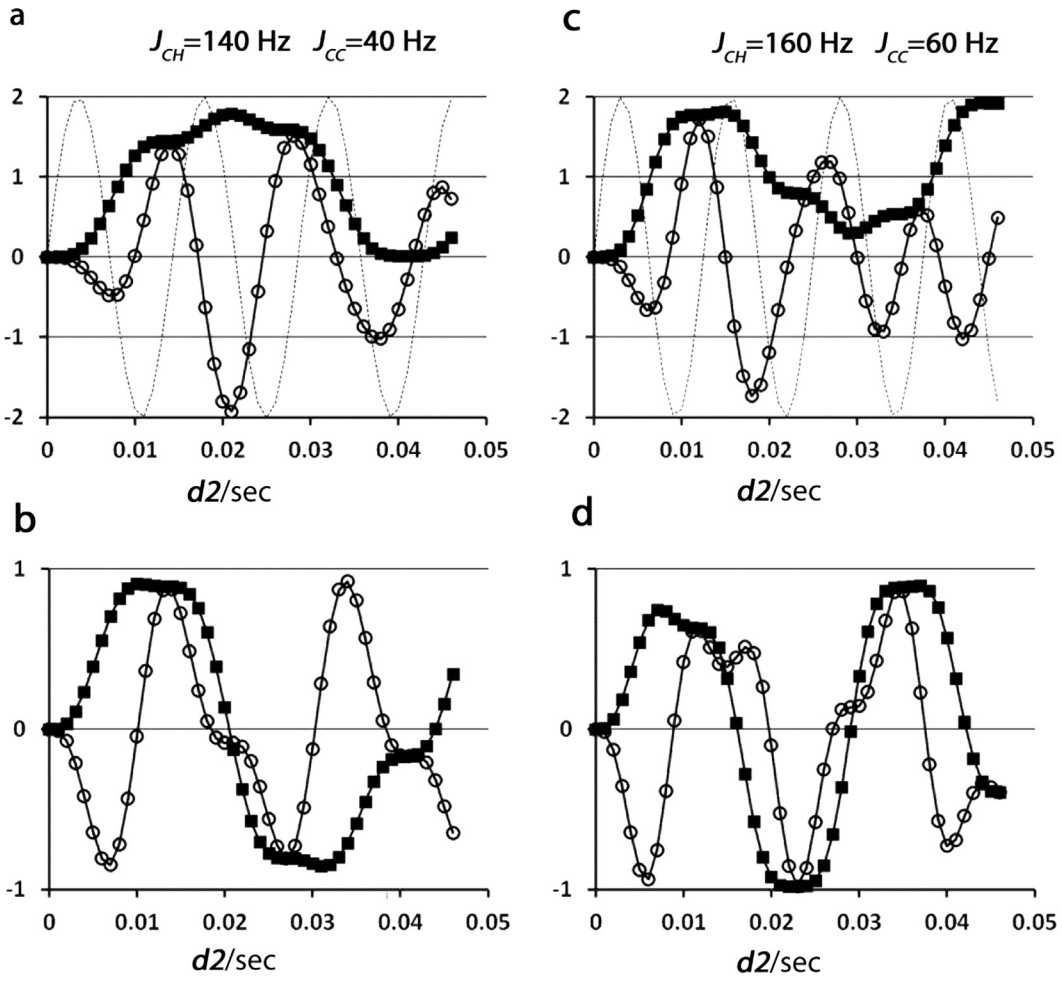

Fig. 2. Amplitudes of carbon double-quantum proton single-quantum coherences as dependent on length of polarization transfer delay *d2*. 2QHMBC – open circles (○), SYMONA – filled squares (■), dashed line - $\sin(\pi J_{CH}t)$. (a) and (c): amplitudes of $\left(C_xC'_x - C_yC'_y\right)(H_x + H'_x)$ coherences; (b) and (d): amplitudes of $\left(C_xC'_x - C_yC'_y\right)2\left(H_yH'_z + H'_yH_z\right)$ coherences; (a) and (b): J_{CH} = 140 Hz, J_{CC} = 40 Hz, J_{HH} = 8 Hz; (c) and (d): J_{CH} = 160 Hz, J_{CC} = 60 Hz, J_{HH} = 8 Hz.

This heteronuclear coupling refocusing is the main difference to the original 2QHMBC since it changes substantially the time development operator during the polarization transfer delay. The polarization transfer period is followed by the (simplified for this task) double-quantum filter made by two carbon pulses with a suitable phase cycling which is in principle similar to that in the standard INADEQUATE experiment [2]. According to Appendix C, Eq. (C3) (Supplementary material 1, Appendices), the coherence $(H_x + H'_x)$ develops to

$$\begin{aligned}&\left(C_xC'_x - C_yC'_y\right)(H_x + H'_x)\left[1 - (c2^s)^2 cos(\pi({}^1J_{CC} + {}^3J_{HH})t)\right.\\&- (s2^s)^2 cos(\lambda^s t)cos(\pi({}^1J_{CC} + {}^3J_{HH})t) - s2^s sin(\lambda^s t)sin(\pi({}^1J_{CC} + {}^3J_{HH})t)\left.\right]\\&+ \left(C_xC'_x - C_yC'_y\right)2\left(H_yH'_z + H'_yH_z\right)\\&\left[(c2^s)^2 sin(\pi({}^1J_{CC} + {}^3J_{HH})t) + (s2^s)^2 cos(\lambda^s t)sin(\pi({}^1J_{CC} + {}^3J_{HH})t)\right.\\&\left.- s2^s sin(\lambda^s t)cos(\pi({}^1J_{CC} + {}^3J_{HH})t)\right],\end{aligned} \tag{2}$$

$$c2^s = \frac{\pi({}^1J_{CH} - {}^2J_{CH})}{\lambda^s},$$

where $s2^s$ and λ^s are defined in Eq. (1). As for 2QHMBC in the previous part this equation and the following text are also valid for ${}^nJ_{CC}$, n = 2, 3,... and corresponding ${}^{n+1}J_{CH}$ and ${}^{n+2}J_{HH}$ couplings. The time dependencies of amplitudes of $\left(C_xC'_x - C_yC'_y\right)(H_x + H'_x)$ and $\left(C_xC'_x - C_yC'_y\right)2\left(H_yH'_z + H'_yH_z\right)$ calculated for typical aliphatic and aromatic system are shown in Fig. 2. A total possible amplitude maximum for $\left(C_xC'_x - C_yC'_y\right)(H_x + H'_x)$ is again two times higher than a maximum for $\left(C_xC'_x - C_yC'_y\right)2\left(H_yH'_z + H'_yH_z\right)$. As each coherence provides the amplitude maxima for different *t*, it is important to search for maximum values, especially of the first member. The simplified expression of Eq. (2) for the amplitude of $\left(C_xC'_x - C_yC'_y\right)(H_x + H'_x)$ coherence is the following:

$$\left(1 - cos(\pi({}^1J_{CC} + {}^3J_{HH})t)\right) \tag{2a}$$

Therefore, the maximum is achieved when $t = 1/({}^1J_{CC} + {}^3J_{HH})$ providing $cos(\pi({}^1J_{CC} + {}^3J_{HH})t) = -1$. Obviously, the first maximum for $\left(C_xC'_x - C_yC'_y\right)(H_x + H'_x)$ amplitude is much broader in comparison with 2QHMBC (see Fig. 2a and c). The simplification in Eq. (2a) is possible as the value of $(s2^s)^2$ is small in practice (about 0.1–0.15) and $(c2^s)^2 = (1 - (s2^s)^2) \sim 0.85$–$0.9$ (for the last equality see Supplementary material 1, Appendices, Appendix A). Specifically, the typical aromatic case provides $(c2^s)^2 = 0.85$, $s2^s = 0.39$ and $(s2^s)^2 = 0.15$. The member $s2^s sin(\lambda^s t)sin(\pi({}^1J_{CC} + {}^3J_{HH})t)$ is small for *t* values in proximity of $1/({}^1J_{CC} + {}^3J_{HH})$ and the rest of the expression is close to a maximum. Therefore, the range of maximum signal intensity is broader, easier to calculate, and the new pulse sequence is less

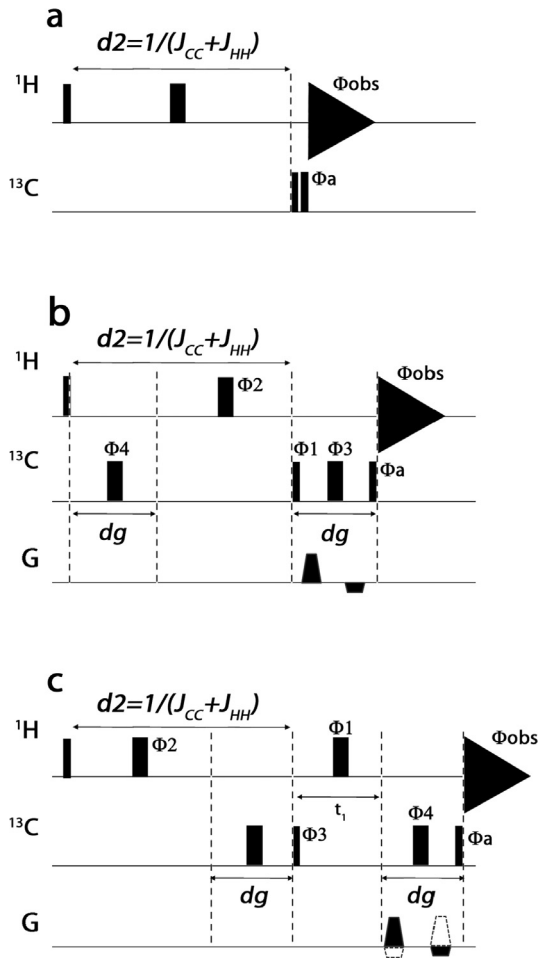

Fig. 3. SYMONA pulse sequence for proton detection of carbon-carbon couplings in symmetric molecules: (a) simplified version of SYMONA (b) 1D SYMONA and (c) 2D SYMONA. The length of the double quantum gradient filter is denoted *dg*, Φa = x, y, −x, −y, Φ1 = (x)4, (−x)4, Φ2 = (x)8, (−x)8, Φ3 = (x)16, (−x)16, Φ4 = (x)32, (−x)32, Φobs = x, −x. Gradient amplitudes are in ratio 3.02:−1 for 1D experiments and in ratios 3.02:−1 and −1:3.02 to get the echo-anti-echo pair for the phase-sensitive 2D experiment.

prone to wrong t values settings than the original 2QHMBC [11]. Contrary to 2QHMBC, this pulse sequence also permits total proton chemical shift refocusing at the beginning of acquisition. Carbon double-quantum coherence develops due to chemical shifts during d3 delay in the 2QHMBC experiment. This can decrease or even nullify the amplitude of $\left(C_xC'_x - C_yC'_y\right)$ term in a density matrix and therefore it can decrease the signal intensity. This is not the case in the new proposed experiment. Another advantageous feature of this pulse sequence is that it, contrary to 2QHMBC, it totally suppresses signals of all spin systems with weakly coupled carbons and weakly coupled protons. Therefore, the obtained spectrum of equivalent carbons does not contain any signals from couplings to other ^{13}C weakly coupled carbons. For the new experiment we propose the acronym SYMONA (SYmmetrical MOlecules Natural Abundance double-quantum experiment).

2.3. Simplified approach

When a time development of proton coherences containing $2C_zC'_z$ products is followed through the preparation period in both sequences, the optimal setting of *d2* delay can be obtained also by simplified consideration. Note that e.g. the double-quantum coherence $\left(C_xC'_x - C_yC'_y\right)(H_x + H'_x)$ arises from the $2C_zC'_z(H_x + H'_x)$ coherence by the first carbon excitation pulse. This pulse creates $2C_yC'_y(H_x + H'_x) = (C_yC'_y - C_xC'_x)(H_x + H'_x) + (C_yC'_y + C_xC'_x)(H_x + H'_x)$. The second term is zero-quantum coherence and it is filtered out by a double-quantum filter.

The initial coherence $(H_x + H'_x)$ is broken at the beginning of the preparation period into two differently developing coherences $(H_x + H'_x)(\frac{1}{2} + 2C_zC'_z)$ and $(H_x + H'_x)(\frac{1}{2} - 2C_zC'_z)$ (see Supplementary material 1, Appendices, Appendices A-C). As the time development of both coherences is a periodic function, both coherences may be captured with the amplitude close to unity but with opposite sign just by choosing the optimal time setting. In favorable cases, the resulting coherence is $[(H_x + H'_x)(\frac{1}{2} + 2C_zC'_z) - (H_x + H'_x)(\frac{1}{2} - 2C_zC'_z)] = (H_x + H'_x)4C_zC'_z$.

In 2QHMBC pulse sequence the first coherence $(H_x + H'_x)(\frac{1}{2} + 2C_zC'_z)$ develops as $cos(\pi(^1J_{CH})t)$ (see Appendices, Appendix B, Eq. (B1), value of $^dJ_{CH} = {}^2J_{CH}$ for measurement of $^1J_{CC}$ is abandoned) while the second coherence $(H_x + H'_x)(\frac{1}{2} - 2C_zC'_z)$ develops as $cos(\pi^1J_{CH}t)cos(\pi^1J_{CC}t)$ (see Supporting Information, Appendices, Appendix B, Eq. (B3), when λ substitutes $\lambda^s \cong \lambda^a$ and is set equal to π^1J_{CH}, and time development by $\tilde{U}^{03}(t)$ is approximated by unity for short times t). The final formula for amplitude of $(H_x + H'_x)2C_zC'_z$ is of $[1 - cos(\pi^1J_{CC}t)]cos(\pi^1J_{CH}t)$, which is close to the approximate Eq. (1a) $[1 - cos(\pi(^1J_{CC} + {}^3J_{HH})t)]\cos(\pi^1J_{CH}t)$. In SYMONA pulse sequence the first coherence $(H_x + H'_x)(\frac{1}{2} + 2C_zC'_z)$ does not develop during *d2* delay at all and the second coherence $(H_x + H'_x)(\frac{1}{2} - 2C_zC'_z)$ is roughly amplitude modulated as $cos(\pi^1J_{CC}t)$ (see Supporting Information, Appendices, Appendix C, where A^{2R} in Eq. (C2) is approximated by unity and time development by $\tilde{U}^{03}(t)$ can be again approximated by unity for short times t). Therefore, the approximate amplitude of $(H_x + H'_x)2C_zC'_z$ coherence is $(1 - cos(\pi^1J_{CC}t))$ which is close to the target amplitude in the approximate Eq. (2a) $(1 - cos(\pi(^1J_{CC} + {}^3J_{HH})t))$. It is important to note that when the $(H_x + H'_x)2C_zC'_z$ coherence is at its maximum then all other coherences are close to their minima (see Supporting Information, Appendices Appendix C, Eq. (C2) or (C3)). Therefore, almost total polarization transfer to $(H_x + H'_x)2C_zC'_z$ can be accomplished in both pulse sequences. The conclusions of this part also apply to cases of $^nJ_{CC}$ and corresponding $^{n+1}J_{CH}$ and $^{n+2}J_{HH}$ couplings, $n > 1$.

2.4. 1D and 2D SYMONA for practical use

Similarly to the original 2QHMBC experiment, the basic version of the SYMONA pulse sequence described above has to be equipped with an effective gradient double-quantum filter for parent signal suppression. Then the SYMONA experiment can be used for recording of 1D spectra (Fig. 3b) or alternatively to obtain 2D phase-sensitive carbon double-quantum chemical shift resolved spectra (Fig. 3c). The cost for recording 2D spectra is one additional refocusing proton pulse. In both sequences the preparation period starts with the proton 90 degrees pulse followed by polarization transfer *d2* delay containing the refocusing proton and carbon inversion pulses to refocus mainly heteronuclear couplings and also proton chemical shift evolution during the preparation period. The polarization transfer period is closed by the first excitation carbon pulse. The total lengths of the polarization transfer period should be roughly set to $1/(^nJ_{CC} + {}^{n+2}J_{HH})$ ($n \geq 1$, see above). The second part of the preparation period consists of *t1* evolution for 2D version and gradient double-quantum filters in both versions. The *t1* evolution delay contains another refocusing proton pulse

in order to refocus heteronuclear couplings and proton chemical shift once more. For detailed description of the time evolution of triple-spin proton single-quantum plus carbon double-quantum coherence, see Supplementary material 1 (Appendices, Appendix D, Eq. (D2)). These coherences develop only under heteronuclear couplings (Supplementary material 1, Appendices, Appendix A, Hamiltonian H^{01}) and proton single-quantum and carbon double-quantum chemical shifts (Hamiltonian H^{00}).

2.5. Experimental results

1,1,2,2-tetrachloroethane (HCl_2C-CCl_2H) (**1**) at natural abundance was chosen as a testing sample. The SYMONA spectrum is depicted in Fig. 4. The wiggly signal in the middle of the spectral pattern at position 0 Hz is a residual parent signal due to an isotopomer with two ^{12}C carbons. The signal of the isotopomer with one ^{13}C and one ^{12}C carbon is totally suppressed. The peaks with negative intensity separated by $(^1J_{CH} + {}^2J_{CH})$ Hz are due to $(\frac{1}{2} + 2C_zC'_z)(H_x + H'_x)$ coherence. The positive signals surrounding each negative peak are separated by $^1J_{CC} + {}^3J_{HH}$ Hz. They originate from the coherence $\left[\left(\frac{1}{2} - 2C_zC'_z\right) + 2\left(C_xC'_x + C_yC'_y\right)\right](H_x + H'_x)$, which appears at the beginning of acquisittion, see Supplementary material 1 (Appendices, Appendix E, Eq. (E4)). The distance between the two inner lines is $\frac{2J^s}{\pi} - (^1J_{CC} + {}^3J_{HH})$ Hz. This spectral pattern appears when $\left(C_xC'_x - C_yC'_y\right)(H_x + H'_x)$ is the prevailing coherence passing through a carbon double-quantum filter (see Supplementary material 1, Appendices, Appendix E, Eq. (E4)) not only for SYMONA but also for the original 2QHMBC. Using $^3J_{HH}$ = 3.0 Hz as obtained from carbon satellites in ^1H spectrum, the resulting value of $^1J_{CC}$ in **1** is 44.5 Hz. Note that if a different value of *d2* delay is used, also $\left(C_xC'_x - C_yC'_y\right)2\left(H_yH'_z + H'_yH_z\right)$ coherence is created and a corresponding spectral pattern based on Eq. (E6) in Supplementary material 1 is proportionally added to the total signal.

Until now the above-mentioned methods were used solely for measurement of compounds with isolated CH-C′H′ fragments [6–9,11,12]. However, there are a number of interesting compounds possessing the CH-C′H′ symmetrical fragment which is unfortunately coupled to other protons. The values of $^1J_{CC}$ couplings for such systems were accessible mainly by computational methods so far. Therefore, the experimental determination can provide important feedback to computational chemists. Fig. 5 presents a 1D SYMONA spectrum of benzene, C_6H_6 (**2**). This compound is a nice example of a complex and very strongly coupled spin system containing a symmetric $H^{13}C$-^{13}CH fragment. The spectral pattern

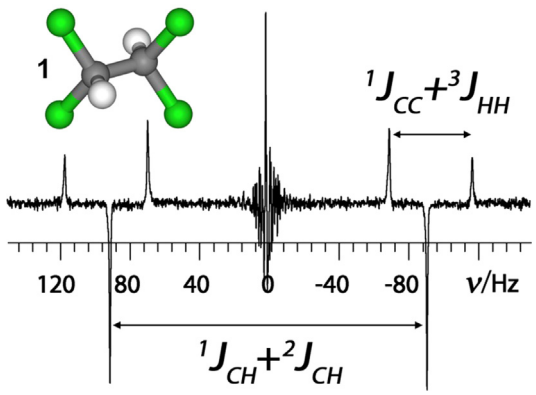

Fig. 4. 1D SYMONA spectrum of 25% (v/v) solution of tetrachloroethane (**1**) in chloroform-d. Polarization transfer delay d2 was 22.72 ms, total experimental time was 53 min with 256 scans.

is basically the same as for an isolated HC-C′H′ spin system. It contains two split negative peaks which are roughly spaced by $(^1J_{CH} + {}^2J_{CH})$ and two pairs of positive peaks on each side of the parent/central peak separated by $(^1J_{CC} + {}^3J_{HH})$ within the pairs. Unfortunately, this basic pattern is split by additional proton-proton homonuclear couplings. Owing to the broad optimum for polarization transfer delay length, the additional proton-proton homonuclear couplings can be neglected in the experimental setting as they are several times smaller than $^1J_{CC}$ and $^1J_{CH}$. Therefore, *d2* can be set to $1/(^1J_{CC} + {}^3J_{HH})$ as for the isolated CH-C′H′ spin system. The $^1J_{CC}$ was chosen to be equal to 55.9 Hz, which was proposed from the measurement in oriented media [4].

In order to derive the corresponding value of $^1J_{CC}$ coupling in **2**, the resulting spectrum has to be simulated since there are no analytical formulas describing similar structures available. The simulated spectrum for **2** is shown in Fig. 5b. Proper simulation requires precise knowledge of all carbon-proton and proton-proton couplings; in the case of benzene, the values can be taken from the paper of Weigert et al. [19] and Laatikainen et al. [20]. The experimental and simulated spectral patterns are not in perfect agreement (Fig. 5a and b). Obviously, the simulation is highly sensitive to selected values of couplings and isotopic chemical shifts. Moreover, the experimental pattern also contains residua of $^3J_{CC}$ and $^2J_{CC}$ couplings from other ^{13}C isotopomers which are not considered in the simulation. The simulation provided the value of $^1J_{CC}$ for benzene close to 56 ± 0.5 Hz, which is in fair agreement with the value 55.9 Hz obtained by Kaski at al. [4].

The influence of additional proton-proton homonuclear couplings is also apparent in the 2D SYMONA spectrum of phenanthrene (**3**). Beside the almost isolated symmetric HC-C′H′ fragment (carbons C7 and C7′) this molecule contains also two fragments with two carbon atoms of accidentally equal chemical shift (atoms C2, C3 and/or C2′, C3′; Fig. 6). The isolated pair C7-C7′ shows a typical pattern for HC-C′H′ system as seen for tetrachloroethane discussed above while the pattern of C2-C3 is multiply split by neighbor protons. The 2D version of the SYMONA experiment was needed since experimental patterns of the two discussed fragments partially overlap. All other signals of weakly coupled carbons were effectively suppressed by SYMONA's polarization transfer delay and by phase cycling of the first 90 deg carbon pulse in the experiment. The determined value of ^1J(C7, C7′) was found to be 62 ± 0.5 Hz. The required value of ^3J(H7, H7′) was obtained from a non-decoupled gHSQC experiment (9 Hz) since ^{13}C satellites of H7-H7′ peak in 1D proton spectrum were buried under neighbor parent proton lines. It was not possible to obtain the value of ^1J(C2,C3) as the simulation did not fit sufficiently the complex spectral pattern despite significant effort.

2.6. $^nJ_{CC}$ couplings over several bonds

For small $^nJ_{CC}$ couplings (n = 2, 3, 4 ...), the value of $s2^s$ (Eq. (1)) achieves just a few hundredths and therefore $s2^s$ can be safely neglected in all equations for such spin systems. Then the exact Eq. (1) and approximate Eq. (1a) for 2QHMBC and exact Eq. (2) and approximate Eq. (2a) for SYMONA are practically identical. Unfortunately, a serious problem arises when the target spins system is affected by additional splitting due to proton homonuclear couplings. When the target $^nJ_{CC}$ coupling is of similar magnitude as the proton-proton homonuclear couplings the signal separation is not sufficient. The additional proton splittings can effectively mask the desired carbon-carbon coupling. Additionally, the important positive multiplets carrying carbon-carbon coupling information are mixed with an intensive negative multiplet which does not contain carbon-carbon coupling information. Therefore, the total signal intensity tends to decrease and carbon-carbon coupling information is dissolved in other signals. Fig. 7 shows a simulated

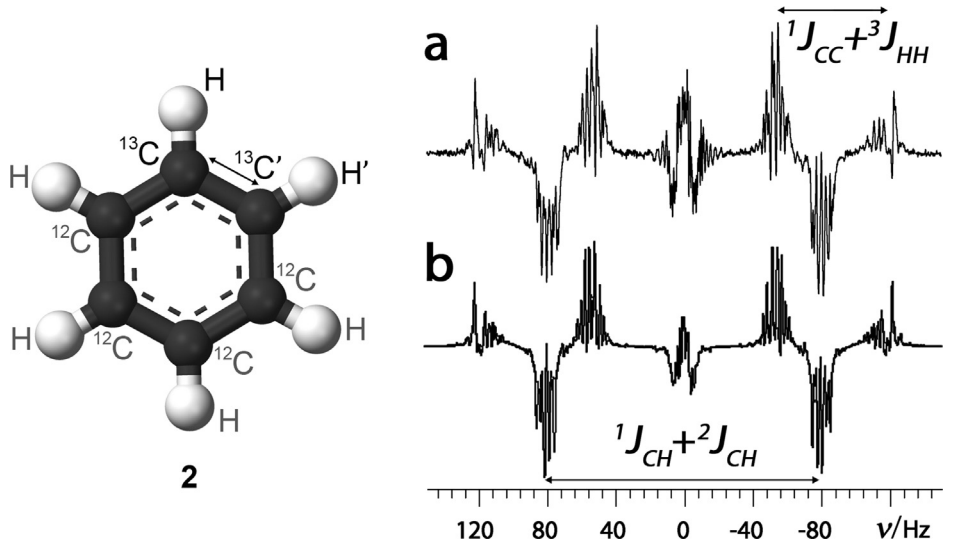

Fig. 5. Experimental (a) and simulated (b) 1D SYMONA spectrum of 25% (v/v) solution of benzene (**2**) in chloroform-d. Polarization transfer delay d2 was 18.18 ms and total experimental time was 3.5 h with 1024 scans.

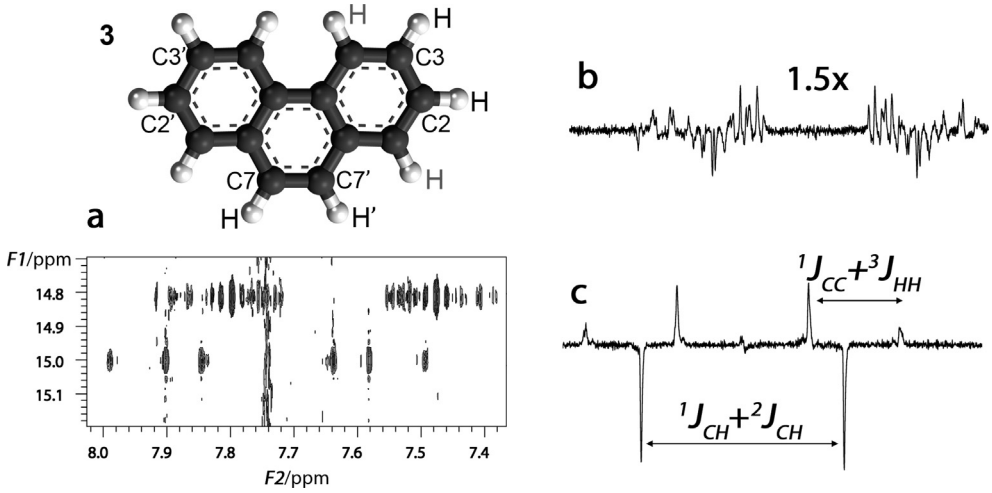

Fig. 6. 2D NMR SYMONA spectrum of saturated solution of phenanthrene in chloroform-d (a), trace for C2-C3 and C2′-C3′ correlation (b), and C7-C7′ correlation (c). Polarization transfer delay d2 was 16.66 ms, spectral width in F1 was 1000 Hz, number of scans per increment 96, number of increments 2 × 32, total number of scans 6144 and total experimental time 21 h.

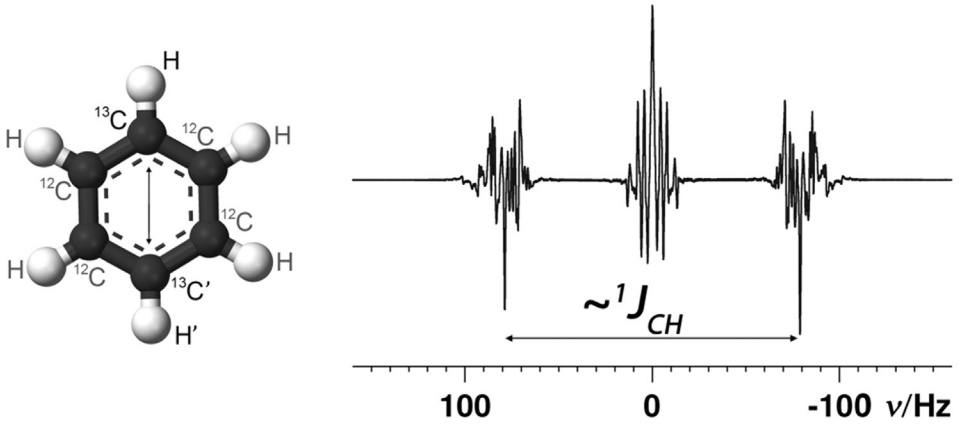

Fig. 7. Simulated 1D SYMONA spectrum of benzene (**2**) isotopomer with two ^{13}C carbons in *para* position. Polarization transfer delay was 100 ms optimized for 10 Hz carbon-carbon coupling.

1D SYMONA spectrum of benzene $^3J_{CC}$ coupling. Obviously, the extraction of the carbon-carbon coupling from such spectral patterns is almost impossible and the obtained value cannot be trustworthy.

2.7. Symmetric CH_2-C′H'_2 case

A very complicated situation arises when a symmetric CH_2-C′H'_2 spin system is considered. The analytical solution of proton single-quantum carbon double-quantum coherence buildup is possible only when significant simplifications are made, e.g. the omission of J_{HH} couplings. In the following all the formulas are written only for one-bond carbon-carbon couplings ($n = 1$) since only for these cases the condition $^nJ_{CC} >> {}^{n+2}J_{HH}$ is satisfied. The full expression of the density matrix at the end of the polarization transfer period just before the first carbon 90-degree pulse can be found in Supplementary material 1 (Appendices, Appendix F). Similarly to the CH-C′H′ spin system, the initial density matrix is divided into two terms: $(H_{x1}+H_{x2}+H'_{x1}+H'_{x2})\left(\frac{1}{2}+2C_zC'_z\right)$ and $(H_{x1}+H_{x2}+H'_{x1}+H'_{x2})\left(\frac{1}{2}-2C_zC'_z\right)$. As shown in Eq. (F5) (Supplementary material 1, Appendices, Appendix F), the first term develops at the end of the polarization transfer period of the original 2QHMBC to

$$(H_{x1}+H_{x2}+H'_{x1}+H'_{x2})\left(\frac{1}{2}+2C_zC'_z\right)\cos\left(\pi({}^1J_{CH}+{}^2J_{CH})t\right) + \left(H_{y1}+H_{y2}+H'_{y1}+H'_{y2}\right)(C_z+C'_z)\sin\left(\pi({}^1J_{CH}+{}^2J_{CH})t\right) \quad (3a)$$

Only the first term is relevant for the creation of double-quantum carbon coherence. Its time dependence is identical to that of the CH-C′H′ spin system (see Supplementary material 1, Eq. (B1)). This coherence does not develop in SYMONA. The second term $(H_x+H_{x2}+H'_{x1}+H'_{x2})\left(\frac{1}{2}-2C_zC'_z\right)$ develops in both methods to a very complex expression (see Supplementary material 1, Appendices, Appendix F, Eq. (F9) and some additional specifications in Eq. (F11) for SYMONA). An exact formula for all density matrix terms with carbon double-quantum coherences passing through the double-quantum filter is not presented here because of a high complexity. Similarly as for the CH-C′H′ spin system, the simplified approach can be applied and only $(H_x+H_{x2}+H'_{x1}+H'_{x2})\left(\frac{1}{2}-2C_zC'_z\right)$ member can be followed for 2QHMBC (see Supplementary material 1, Appendices, Appendix F, Eq. (F9)).

$$(H_{x1}+H_{x2}+H'_{x1}+H'_{x2})\left(\frac{1}{2}-2C_zC'_z\right)\left(\frac{3}{4}Re\left(A^{M1}\right)+\frac{1}{4}Re\left(A^{M2}\right)\right) = (H_x+H_{x2}+H'_{x1}+H'_{x2})\left(\frac{1}{2}-2C_zC'_z\right) \times\left[\frac{3}{4}\left(\cos\left(\lambda^{m1}t\right)\cos\left(\pi^1J_{CC}t\right)+s2^{m1}sin\left(\lambda^{m1}t\right)sin\left(\pi^1J_{CC}t\right)\right) +\frac{1}{4}\left(\cos\left(\lambda^{m1}t\right)\cos\left(\lambda^{m2}t\right)+\left(c2^{m1}c2^{m2}+s2^{m1}s2^{m2}\right)sin\left(\lambda^{m1}t\right)sin\left(\lambda^{m2}t\right)\right)\right], \quad (3b)$$

$$\lambda^{m1}=\pi\sqrt{\left(({}^1J_{CH}-{}^2J_{CH})^2+{}^1J_{CC}^2\right)},\lambda^{m2}=\pi\sqrt{\left(4({}^1J_{CH}-{}^2J_{CH})^2+{}^1J_{CC}^2\right)},$$

$$s2^{mi}=\pi\frac{|{}^1J_{CC}|}{\lambda^{mi}},\ i=1,\ 2, c2^{m1}=\pi\frac{({}^1J_{CH}-{}^2J_{CH})}{\lambda^{m1}},$$

$$c2^{m2}=2\pi\frac{({}^1J_{CH}-{}^2J_{CH})}{\lambda^{m2}}.$$

Considering Eqs. (3a) and (3b) we get for the amplitude of $(H_{x1}+H_{x2}+H'_{x1}+H'_{x2})2C_zC'_z$ equal to

$$\cos\left(\pi({}^1J_{CH}+{}^2J_{CH})t\right)-\left[\frac{3}{4}\left(\cos\left(\lambda^{m1}t\right)\cos\left(\pi^1J_{CC}t\right)+s2^{m1}sin\left(\lambda^{m1}t\right)sin\left(\pi^1J_{CC}t\right)\right) +\frac{1}{4}\left(\cos\left(\lambda^{m1}t\right)\cos\left(\lambda^{m2}t\right)+\left(c2^{m1}c2^{m2}+s2^{m1}s2^{m2}\right)sin\left(\lambda^{m1}t\right)sin\left(\lambda^{m2}t\right)\right)\right]\cong$$

$$\cos\left(\pi({}^1J_{CH}+{}^2J_{CH})t\right) -\frac{3}{4}\left(\cos\left(\lambda^{m1}t\right)\cos\left(\pi^1J_{CC}t\right)+s2^{m1}sin\left(\lambda^{m1}t\right)sin\left(\pi^1J_{CC}t\right)\right) -\frac{1}{4}\cos\left[(\lambda^{m2}-\lambda^{m1})t\right] \quad (3c)$$

The last equality emerges from the fact that $\left(c2^{m1}c2^{m2}+s2^{m1}s2^{m2}\right)\cong 1$.

The result is very similar to the amplitude of $(H_x+H'_x)\left(C_xC'_x-C_yC'_y\right)$ in Eq. (1). The main difference is the minor term $\frac{1}{4}\cos\left[(\lambda^{m2}-\lambda^{m1})t\right]$. Remember that Eqs. (3b) and (3c) are approximate not only because of the simplification made above but also due to the neglect of the J_{HH} coupling.

Using the same simplification the $(H_{x1}+H_{x2}+H'_{x1}+H'_{x2})\left(\frac{1}{2}-2C_zC'_z\right)$ in SYMONA pulse sequence develops to:

$$(H_{x1}+H_{x2}+H'_{x1}+H'_{x2})\left(\frac{1}{2}-2C_zC'_z\right)\left(\frac{3}{4}Re\left(A^{2RM1}\right)+\frac{1}{4}Re\left(A^{2RM2}\right)\right). \quad (3d)$$

Here A^{2RM1} and A^{2RM2} are defined in Eq. (F11) (Supplementary material 1, Appendices). When the simplified versions of A^{2RM1} and A^{2RM2} in Eq. (F11a) are considered and if the non-developing $(H_{x1}+H_{x2}+H'_{x1}+H'_{x2})\left(\frac{1}{2}+2C_zC'_z\right)$ coherence is included, the amplitude of $(H_{x1}+H_{x2}+H'_{x1}+H'_{x2})2C_zC'_z$ becomes

$$\frac{3}{4}\left(1-\cos\left(\pi^1J_{CC}t\right)\right) \quad (3e)$$

If $c2^{m1}$ and $c2^{m2}$ are approximated by unity in Eq. (F11a).

The obtained approximate Eqs. (3c) and (3e) show that the polarization transfer behavior of the CH_2-C′H'_2 spin system is rather similar to that in the CH-C′H′ spin system.

Fig. 8 shows the experimental and simulated SYMONA spectrum of dichloroethane (**4**) CH_2Cl-CH_2Cl. The two negative single lines arising due to $(H_x+H_{x2}+H'_{x1}+H'_{x2})\left(\frac{1}{2}+2C_zC'_z\right)$ coherence are spaced by $({}^1J_{CH}+{}^2J_{CH})$ Hz, as in the CH-C′H′ case. The negative peak in the center of the experimental spectrum is a residuum of a parent peak. The positive signals containing carbon-carbon coupling information are more split than for the CH-C′H′ case and the signal intensity is lower. Therefore, longer experimental time is necessary, specifically 3.4 h. The proton-proton and carbon-proton couplings were extracted by simulation of carbon satellites in a proton spectrum and by simulation of a non-decoupled carbon spectrum, respectively. A value of 39 Hz for $^1J_{CC}$ was obtained from the simulation of the SYMONA experiment.

3. Conclusions

Analytical formulas for time development of density matrix in 2QHMBC experiment applied for detection of carbon-carbon couplings in symmetrical HC-C′H′ molecular fragments were deduced. Based on derived formulas, the polarization transfer delay can be optimized in order to get the maximum signal intensity. Additionally, a new pulse sequence called SYMONA (SYmmetrical MOlecules Natural Abundance double-quantum experiment) was proposed and tested on real samples. The range of maximum signal intensity in the SYMONA experiment is broader and easier to predict. Therefore, it is less prone to a wrong setting of polarization

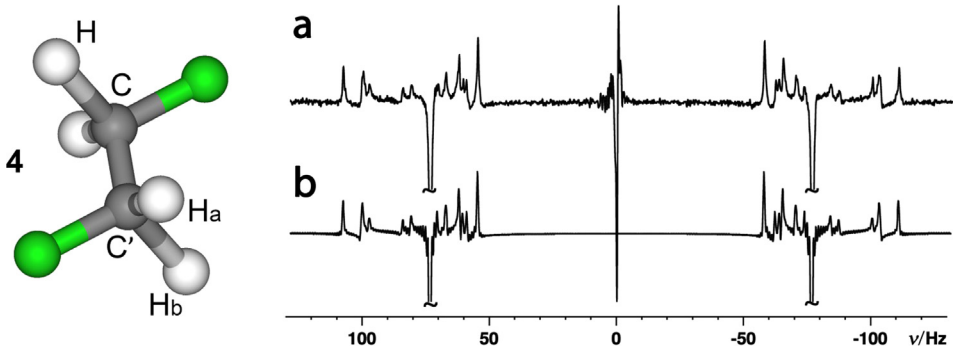

Fig. 8. Experimental (a) and simulated (b) SYMONA spectrum of symmetrical dichloroethane (25% solution (v/v) in chloroform-d) (**4**). Polarization transfer delay d2 = 20 ms. Experimental spectrum was acquired with 1024 scans. The following values were used for spectrum simulation: $^{1}J_{CH}$ = 153.5 Hz, $^{2}J_{CH}$ = −3.4 Hz, $^{2}J_{HH}$ = −14 Hz, $^{3}J_{HHa}$ = 8.0 Hz, $^{3}J_{HHb}$ = 6.0 Hz.

transfer delay length than the original 2QHMBC and can be applied to more complicated spin systems. However, the determination of couplings in the HC-C′H′ system coupled to other protons and H_2C-C′H'_2 is complicated by additional splitting due to proton-proton homonuclear couplings and requires thorough simulation. It was also shown that the additional splitting by proton-proton homonuclear couplings prevents the determination of $^{n}J_{CC}$ couplings over more bonds by both 2QHMBC and SYMONA experiments.

4. Experimental

All simulations were performed using Bruker NMRSIM [21] simulation package. All simulations were performed with 4 scans for 1D spectra and with 4 scans for each FID in 2D spectra. All experimental results were obtained on a Varian/Agilent Unity 500 MHz NMR spectrometer. All the liquid samples were in 25% (v/v) concentration in chloroform-d $CDCl_3$, a phenanthrene sample was used as saturated solution in chloroform-d. The NMR experiments were carried out on a 5 mm PFG indirect detection probe at 25 °C, with relaxation delay 10 s, acquisition time 2 s, FIDs were zero-filled from two to four times the number of acquired points, gradient pulses and gradient stabilization delays were both 1 ms long, rectangular gradient pulses were used with amplitudes 32 G/cm and 10.67 G/cm, proton 90 degree pulses and carbon 90 degree pulses were 4.2 μs and 28 μs, respectively. Note that the gradients ratio should be $(2\gamma_C + \gamma_H):(2\gamma_C - \gamma_H) = 3.02:-1$. The originally proposed ratio [11] 3:−1 is not exact and may cause severe signal attenuation for stronger gradients. Source codes for 1D SYMONA and 2D SYMONA pulse sequences for Bruker or Varian/Agilent NMR spectrometers are included in the Supplementary materials 2, 3, 4, and 5, files SYMONA1D-Bruker, SYMONA2D-Bruker, SYMONA1D-Varian and SYMONA2D-Varian.

Acknowledgments

This work was supported by the Czech Science Foundation (grant No. 15-12719S).

Appendix A. Supplementary material

Supplementary data associated with this article can be found, in the online version, at https://doi.org/10.1016/j.jmr.2018.12.002.

References

[1] Part B and Part C in:M. Kaupp, M. Bühl, V. G. Malkin (Eds), Calculation of NMR and EPR Parametres Wiley, Weinheim, 2004, pp. 85–462.
[2] A. Bax, R. Freeman, S.P. Kempsell, Natural abundance ^{13}C–^{13}C coupling observed via double-quantum coherence, J. Am. Chem. Soc. 102 (1980) 4849–4852.
[3] B. Reif, M. Köck, R. Kerssebaum, H. Kang, W. Fenical, C. Griesinger, ADEQUATE, a new set of experiments to determine the constitution of small molecules at natural abundance, J. Magn. Reson. A 118 (1996) 282–285.
[4] J. Kaski, J. Vaara, J. Jokisaari, ^{13}C–^{13}C spin-spin coupling tensors in benzene as determined experimentally by liquid crystal NMR and theoretically by *ab Initio* calculations, J. Am. Chem. Soc. 118 (1996) 8879–8886.
[5] P.L. Corio, Structure of high-resolution NMR spectra, Academic Press, New York, London, 1966.
[6] S. Berger, The use of proton-coupled INADEQUATE to determine carbon-carbon spin coupling constants in symmetrical molecules, J. Magn. Reson. 66 (1986) 555–557.
[7] K. Kamieńska-Trela, L. Kania, J. Sitkowski, E. Bednarek, Analysis of spectral parameters of *trans*- and *cis*-silyl substituted 1,2-dihalogenoethenes including one-bond CC spin-spin coupling constants across double bonds, J. Orgmet. Chem. 364 (1989) 29–38.
[8] M. Witanowski, Z. Biedrzycka, Spin-spin couplings between ^{13}C nuclei in five-membered heteroaromatic ring systems, Magn. Reson. Chem. 32 (1994) 62–66.
[9] K. Hassler, E. Hengge, F. Schrank, M. Weidenbruch, SiSi-Kopplungskonstanten symmetrischer disilane, Spectrochim. Acta 47A (1991) 57–62.
[10] A. Meissner, D. Moskau, N.C. Nielsen, O.W. Sorensen, Proton-detected ^{13}C–^{13}C double-quantum coherence, J. Magn. Reson. 124 (1997) 245–249.
[11] S. Berger, Proton detection of carbon-carbon spin coupling constants in symmetrical molecules, J. Magn. Reson. 142 (2000) 136–138.
[12] S. Berger, A. Krebs, B. Thölke, H. Siehl, Experimental and quantum chemical investigation of the stereochemical dependence of spin coupling constants in symmetrical strained alkenes, Hans-Ullrich Sielhl, Magn. Reson. Chem. 38 (2000) 566–569.
[13] J.H. Ardenkjaer-Larsen, B. Fridlund, A. Gram, G. Hansson, L. Hansson, M.H. Lerche, et al., Increase in signal-to-noise ratio of >10,000 times in liquid-state NMR, Proc. Natl. Acad. Sci. USA 100 (2003) 10158–10163.
[14] M.H. Levitt, Singlet and Other States with Extended Lifetimes, in: D.M. Grant, R.K. Harris (Eds.), Encyklopedia of Magnetic Resonance, vol. 10, John Wiley & Sons Ltd, 2010.
[15] Y. Feng, R.M. Davis, W.S. Warren, Accessing long-lived nuclear singlet states between chemically equivalent spins without breaking symmetry, N. Phys. 8 (2012) 831–837.
[16] T. Theis, Y. Feng, T. Wu, W.S. Warren, Composite and shaped pulses for efficient and robust pumping of disconnected eigenstates in magnetic resonance, J. Chem. Phys. 140 (2014), 014201–1-014201–7.
[17] K. Claytor, T. Theis, Y. Feng, W. Warren, Measuring long-lived 13C2 state lifetimes at natural abundance, J. Magn. Reson. 239 (2014) 80–86.
[18] T. Theis, M. Truong, A.M. Coffey, E.Y. Chekmenev, W.S. Warren, LIGHT-SABRE enables efficient in-magnet catalytic hyperpolarization, J. Magn. Reson. 248 (2014) 23–26.
[19] F.J. Weigert, J.D. Roberts, Nuclear magnetic resonance spectroscopy. Benzene-^{13}C, J. Am. Chem. Soc. 89 (1967) 2967–2969.
[20] R. Laatikainen, J. Ratilainen, R. Sebastian, H. Santa, NMR study of aromatic-aromatic interactions for benzene and some other fundamental aromatic systems using alignment of aromatics in strong magnetic field, J. Am. Chem. Soc. 117 (1995) 11006–11010.
[21] NMR-SIM in TopSpin 3.2 PL7 for Windows 7, Bruker BioSpin, Rheinstetten.